Seasonal Solar Thermal Energy Storage using Thermochemical Sorption in Domestic Dwellings in the UK

Zhiwei Ma, Huashan Bao*, Anthony Paul Roskilly

Sir Joseph Swan Centre for Energy Research, Newcastle University, Newcastle upon Tyne, NE1 7RU, UK

Abstract

The present paper explored the potential of the seasonal solar thermal energy storage (SSTES) system using ammonia-based chemisorption for domestic application in the UK. The dynamic charging/discharging performance of the SSTES has been simulated using the real weather data with the solar thermal collector models, the domestic heating demand model and the chemisorption model. The selection of working salts has significantly influence on the system design and dynamic performance. The $CaCl_2$-4/8NH_3 chemisorption can satisfy almost 100% of space heating demand when using low temperature hating facility during discharging stage, however, due to its relatively higher desorption temperature and limited sunlight available in the Newcastle-upon-Tyne the required solar collectors area exceeds the commonly available space of dwelling roof. The NaBr-0/5.25NH_3 chemisorption is only able to contribute 18.6% of heating demand because the temperature of the discharged heat cannot reach the required level for most of the time in the heating season. The best scenario studied was using $BaCl_2$-0/8NH_3 chemisorption SSTES (45.2 m^3) combined with low temperature heating facilities and a 30.5 m^2 solar collector, which can cover about 60.3% of space heating for a dwelling with a heat loss coefficient at 150 W/K.

Keywords: Thermochemical Sorption; Seasonal Solar Thermal Energy Storage; Solar Heat; Domestic Heating Demand; Simulation

* Corresponding author. Tel.: +44 001912084849; Fax: +44 001912226920;
E-mail address: huashan.bao@ncl.ac.uk

Nomenclature

Ar	parameter in chemisorption kinetic model (s^{-1})
c_p	specific heat (J/(kg K))
D	diameter (m)
h	heat transfer coefficient (W/(m^2 K))
ΔH	reaction enthalpy (J/mol NH_3)
I	solar radiation (W/m^2)
L	length (m)
m	parameter in chemisorption kinetic model (-)
M	mass (kg)
n	molar number (mol)
Nu	Nusselt number (-)
P	pressure (Pa)
$P°$	standard pressure (Pa)
Pr	Prandtl number (-)
Q	heating load (kWh)
r	radius (m)
Re	Reynolds number
S	source term (W/m^3)
ΔS	reaction entropy (J/(mol K))
t	time (s)
T	temperature (K)
u	flow velocity (m/s)
$\overline{UA}$	overall heat loss coefficient of dwelling (W/K)
V	volume (m^3)
x	degree of conversion (-)

Greeks

δ	thickness (m)
η	efficiency (-)
λ	thermal conductivity (W/(m K))
ρ	density (kg/m^3)
Subscripts	
a	ambient
ad	adsorption / adsorbent
b	bulk
c	constraint
de	desorption
eq	equilibrium
f	heat transfer fluid
in	inlet
NH3	ammonia
R	room
SH	space heating

1 Introduction

In the UK, about 82.8% of domestic final energy consumption is for space and water heating; the total space and water heating consumes about 33.9% of the final energy consumption of the UK economy, which is about 48 Mt oil equivalent annually [1]. To reduce greenhouse gas emissions and improve energy security, it is imperative to promote the development of low carbon heating technologies with higher energy efficiency and encourage higher penetration of renewable energy source.

The UK receives a moderate amount of sunlight, with an insolation of between 0.8 and 1.3 megawatt-hours per square meter (MWh/m^3) [2], and the amount of solar radiation incident on the roof of a typical home exceeds its energy consumption over a year [3]. However, the longstanding barriers to utilise the solar thermal energy lie in the mismatch between the solar energy availability and the heating demand, which has motivated intensive research and development of seasonal solar thermal

energy storage (SSTES) [3]. Some large scale water based SSTES system has been demonstrated [4, 5]. These systems stored hot water in tank, pit, borehole or aquifer layer for community-scale district heating, and the energy storage density was at the level of 50 kWh/m^3. Small scale SSTES systems, e.g. for a single dwelling, have not yet been fully investigated, considering the risk of large volume system employing the conventional sensible heat storage method, which is not favourable in the domestic scenarios.

Ammonia-based chemisorption has been widely recognized as a promising thermal energy storage technology [6] due to its large energy density and almost zero-loss long-term storage, it has great potential for the compact domestic SSTES application. Ma et al. [7] studied the feasibility of applying SSTES system in domestic dwellings in eight representative cities in the UK. Storage capacities and system volumes of different storage technologies and the critical solar collector areas required to meet the heating demand were studied and compared. When the overall heat loss coefficient of the dwelling was 150 W/K and water inlet temperature to the solar collector was 40 °C, the critical solar collector area and storage capacity of a thermochemical sorption SSTES were in the range of 33.51–34.29 m^2 and 6073.25–6336.35 kWh respectively. Li et al. [8, 9] proposed a dual-mode ammonia chemisorption cycle for SSTES using two sets of reactor-condenser/evaporator units. During warm winter with relatively higher ambient temperature, ambient heat was used to evaporate ammonia and the ammonia vapour was adsorbed by the salt in reactor to discharge the stored heat; while in the cold winter, when one-stage chemisorption was not enough to deliver the heat at sufficient high temperature for space heating, the heat released from one ammonia chemisorption unit was used to evaporate the ammonia for the other chemisorption unit as the second-stage heat upgrading. Using this method, the storage system can deliver useful heat under the weather condition of −30°C to 15°C ambient temperature in the winter. The storage efficiency and energy density were at 0.6 and 1043 kJ/kg (material-based) salt when using $CaCl_2$-NH_3 as the working pair with the targeted output heat temperature at 62 °C and ambient temperature at 0 °C. The main drawback of this approach is the potentially further reduced system-based energy density of the SSTES due to more complex system configuration and more components involved. Jiang et al. [10] experimentally studied the SSTES system using resorption $MnCl_2$-$CaCl_2$-NH_3 working pair. The system featured a specific energy

density of 1149 kJ/kg (material-based) and a storage efficiency of 0.58 when the charging heat temperature, ambient temperature and output temperature were at 150 ℃, 15 ℃ and 30 ℃ respectively. The authors also gave two possible solutions to elevate the output temperature during discharging stage, one was using the concept proposed by Li et al. [8, 9] to upgrade the heat using two-stage adsorption, the other was introducing electricity to compress the desorbed low pressure ammonia to a higher pressure level which then can be adsorbed by the salt at relatively higher temperature.

Some studies have been done on SSTES using ammonia-based chemisorption, however there is lack of dynamic performance simulation of the whole system to be applied to a real world scenario. To go beyond the theoretical analysis and equilibrium performance discussion devoiced from the real condition of the climate and the solar sources, and get better understanding and more insights of system design and material selection in practice, the current work presents a case study of demonstrating the feasibility of thermochemical sorption SSTES system in the city of Newcastle-upon-Tyne in the UK, through numeric simulation of system dynamic behaviour using the real climate data. The mathematical model of the whole thermochemical sorption (i.e. chemisorption) SSTES system integrates the models of two different types of solar collectors (flat-plate type and evacuated tube type), space heating demand model and the chemisorption model to calculate the maximum amount of heat to be charged and discharged and the share of the total heating demand can be delivered by the SSTES, as well as the corresponding SSTES volume and the solar collector area required.

2 Analysis methods

2.1 Chemisorption SSTES system

The basic configuration of a chemisorption system, which comprises one adsorbent reactor and one refrigerant container (condenser/evaporator), is applied in this work as shown in Figure 1. The shell-and-finned tube type of the adsorbent reactor was employed as the adsorbent is compressed and packed in between the fins gap while the heat transfer fluid flows inside the tubes. Each finned tube is treated as one chemisorption module, thereby the whole system can be easily scaled up or down by

adding more or removing some modules. The halide salt ammoniate-ammonia coordination reaction of $CaCl_2$-4/8NH_3, $BaCl_2$-0/8NH_3 and NaBr-0/5.25NH_3 were used for chemisorption in the present study due to their relatively low desorption temperature [11] so that to allow the effective recovery and utilisation of solar thermal energy from two most common types of solar collectors, flat-plate collector and evacuated tube collector.

During the charging process, the adsorbent in the SSTES is heated and desorbs ammonia vapour, namely, the hot water heated by the solar collector supplies heat to a group of modular adsorbent finned-tubes and subsequently moves to another group when the desorption of the previous group completes. The number of each group of modular finned-tubes has been analyzed and discussed to find out whether there is an optimal arrangement. The desorbed ammonia is then condensed in the condenser at ambient temperature. Because of the varying weather condition including the solar radiation as the heat sources and the ambient temperature as the heat sink temperature, both of the obtained hot water temperature and the required desorption temperature are changing, therefore the thermal charging via ammonia desorption unnecessarily occurs continuously but only when the temperature of the heated adsorbent goes beyond the desorption equilibrium temperature determined by the ammonia condensation pressure.

During the discharging process, the condenser becomes an evaporator. The ammonia evaporates at the ambient temperature and subsequently is adsorbed by a group of modular adsorbent finned-tubes, while the adsorption heat released is used to heat the circulating water for space heating; when the adsorption of this group completes, the evaporated ammonia vapour is directed to another group of adsorbent finned-tubes to continue releasing adsorption heat, and so on. The feed and return temperature of the hot water for space heating were pre-defined based on different end-user heating facilities, such as conventional radiator using 70 °C as feed temperature and 40 °C as return temperature [12] and the low temperature heating facility (e.g. floor heating or fan convector) using 35 °C as feed temperature and 25 °C as return temperature [13]. If the total heating demand is known, thus the hot water flow rate at the end-user heating facility would be a fixed value for satisfactory heating, with the pre-defined temperature of the feed and return water; further, the water flow rate through each modular finned-tube depends on the number of the modular tubes in each group. Ideally,

the chemisorption SSTES is supposed to cover the entire space heating demand in winter, however this strongly relies on the practical operating condition, i.e. the weather condition in the winter. Because: (1) the chemisorption temperature is pressure dependant due to the fixed mono-variant equilibrium which implies the reaction can occur at a higher temperature if the sorption pressure is higher, or occur at a low temperature conversely; (2) the sorption pressure is dominated by the evaporation pressure and the evaporation is determined by the ambient temperature; (3) the real ambient temperature is highly varying throughout the discharging period. If the ambient temperature is too low to drive exothermic adsorption at the desired temperature level, then the studied SSTES is incompetent to solely cover the whole heating demand but requires supplementary heat from i.e. a back-up boiler. In this instance, the solution conceived in this study is to have the return water from the end-user heating facility flowing through the chemisorption storage system first to collect the adsorption heat as much as possible; and then heading to the solar collector to recover solar heat if there is any available during winter time; eventually being heated by a back-up boiler to ensure the delivered hot water temperature as desired. Then the ratio of the coverage by the chemisorption SSTES will be evaluated and discussed, which is defined as the percentage of the useful heat delivered by the SSTES to the total space heating demand.

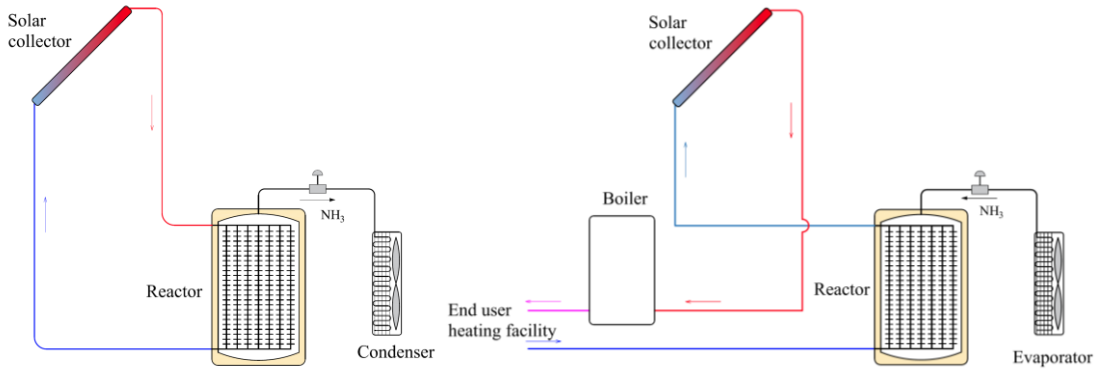

(a) **(b)**

Figure 1 Schematic diagram of chemisorption SSTES system, (a) charging process; (b) discharging process.

2.2 Useful solar heat on roof

The hourly weather data of Newcastle-upon-Tyne, including atmospheric temperature and global horizontal radiation, is available from the software Meteonorm, as shown in Figure 2. The solar irradiance projected to a solar collector which is 45° tilted and facing south has been calculated and reported in our previous study [7]. The roof area for solar collector installation is in the range of 16.5-31.0 m^2 for the majority of domestic dwellings in the UK [14], so the value of 20 m^2, which represents the average semi-detached house roof area, was assumed as the solar collector area in the charging process of the current study.

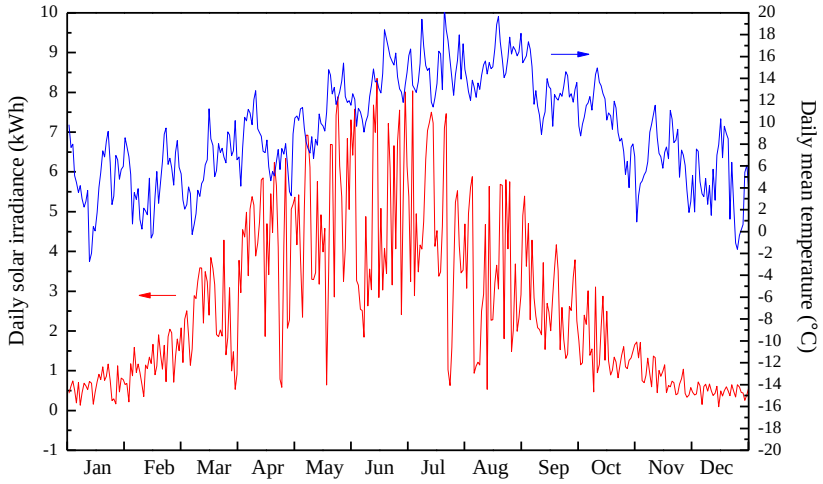

Figure 2 Daily solar irradiance and mean temperature of Newcastle upon Tyne, available from Meteonorm.

The collector thermal efficiency was used to determine the useful solar heat gained by the heat transfer fluid (water in current study) flowing through solar collectors. Empirical correlations of thermal efficiencies of the flat-plate collector and the evacuated tube collector, as the functions of solar irradiance and temperature difference between inlet water and ambient, were developed based on dozens of tested results reported in [15]:

Flat-plate collector (Selective Coating)

$$\eta = 0.662833 - 3.61063\frac{T_{\mathrm{in}} - T_{\mathrm{a}}}{I} - 0.01143\frac{(T_{\mathrm{in}} - T_{\mathrm{a}})^2}{I} \quad (1)$$

Evacuated tube collector

$$\eta = 0.4739 - 1.37522\frac{T_{\mathrm{in}} - T_{\mathrm{a}}}{I} - 0.0049\frac{(T_{\mathrm{in}} - T_{\mathrm{a}})^2}{I} \quad (2)$$

(Sputtered aluminium nitride)

2.3 Domestic heating demand

The hourly space heating demand Q_{SH} in the unit of kWh of a typical dowelling in the UK was estimated based on the following equation [7]:

$$Q_{SH} = \frac{\overline{UA}(T_R - T_a) * 3600}{1000 * 3600} = \overline{UA}(T_R - T_a)/1000 \quad (3)$$

where $\overline{UA}$ is the overall heat loss coefficient in the unit of W/K, T_R is the room temperature and T_a is the ambient temperature. The value of $\overline{UA}$ depends on many factors, such as the dwelling floor area, the insulation conditions, the opening state of the windows, the living behaviour of the occupants, the exterior wind speeds and so on. This value has been measured and reported by literature [16, 17] in the range of 50 W/K to 300 W/K for the UK dwellings. A value of 150 W/K was used in the current study to represent an ordinary UK semi-detached dwelling. The room temperature (T_R) was assumed to be maintained at 21 °C throughout the thermal discharging period.

2.4 Chemisorption model and simulation

The model of the modular finned-tube reactor/heat exchanger with adsorbent filled in between the fins and water flowing inside the tube was developed. The following assumptions were used to simply the modelling:

- The thermal mass of ammonia was negligible;
- Thermal loss from the reactor was ignored;
- The non-equilibrium performance of chemisorption was evaluated at an equilibrium pressure drop of 1.0 bar;
- The mass transfer limitation was ignored in the chemisorption;

Table 1 Parameters of the modular chemisorption reactor.

Parameters	Values

Tube inner radius, r_f, (mm)	10
Tube outer radius, r_f, (mm)	12
Fin radius, r_s, (mm)	75
Fin thickness, δ, (mm)	1
Fin number, n_{fin}, (-)	100
Length, L, (mm)	1500
Adsorbent bulk density, ρ_b, (kg/m^3)	450
Adsorbent mass, m_{ad}, (kg)	10.848
Adsorbent bulk volume, V_{ad}, (m^3)	0.024
Expanded graphite mass ratio, f, (-)	0.25

Figure 3 shows the physical model of the modular finned-tube reactor and the used parameters are given in Table 1. The heat conduction equations for the tube, fins and adsorbent is given as

$$\rho c_p \frac{\partial T}{\partial t} = \frac{1}{r}\frac{\partial}{\partial r}\left(r\lambda\frac{\partial T}{\partial r}\right) + \frac{\partial}{\partial z}\left(\lambda\frac{\partial T}{\partial z}\right) + S \tag{4}$$

where S is the source term representing the chemisorption reaction heat which only applicable to adsorbent and can be calculated by the following equation:

$$S = \frac{n_{\mathrm{NH_3}}}{V_b}\frac{dx}{dt}\Delta H \tag{5}$$

where x is the degree of conversion of the chemisorption, which is from 1 to 0 during desorption and from 0 to 1 during adsorption; ΔH is the chemisorption enthalpy change at the unit of J/mol NH_3; n_{NH3} is the total mole of ammonia that can be desorbed/adsorbed; V_b is the bulk volume of the adsorbent. The following classic chemisorption kinetic equations are used for ammonia adsorption and desorption respectively in the current study [18]:

$$\frac{\mathrm{d}x}{\mathrm{d}t} = Ar_{\mathrm{ad}}(1-x)^{m_{\mathrm{ad}}}\frac{P_c - P_{\mathrm{eq}}(T)}{P_c} \tag{6a}$$

$$\frac{\mathrm{d}x}{\mathrm{d}t} = Ar_{\mathrm{de}}x^{m_{\mathrm{de}}}\frac{P_c - P_{\mathrm{eq}}(T)}{P_c} \tag{6b}$$

where P_c is the constraint pressure of the chemisorption and is (P_{NH3} − 1) bar in adsorption and (P_{NH3} + 1) in desorption according to the assumption of 1 bar equilibrium pressure drop. The calculation of P_{eq} (T) was based on the following van't Hoff equation [19]

$$\ln \frac{P_{eq}(T)}{P^{\circ}} = -\frac{\Delta H}{RT} + \frac{\Delta S}{R} \quad (7)$$

where P° is the standard pressure (1 bar), ΔH and ΔS are reaction enthalpy and entropy changes. ΔH and ΔS as well as specific heats of the used salts are listed in Table 2.

Table 2 Enthalpy and entropy changes of ammonia chemisorption, and specific heat of the used salts.

	ΔH (J/mol NH_3)	ΔS (J/(mol K))	c_p (J/(kg K)) [21]
$CaCl_2$-4/8NH_3	41013 [19]	230.30 [19]	$\frac{4.184}{M} \times (16.9 + 0.00386 \times T(K))$
$BaCl_2$-0/8NH_3	37665 [19]	227.25 [19]	$\frac{4.184}{M} \times (17.0 + 0.00334 \times T(K))$
NaBr-0/5.25NH_3	30491 [20]	208.8 [20]	$\frac{4.184}{M} \times (11.74 + 0.00233 \times T(K))$

The above kinetic equations have been widely used for ammonia-based chemisorption with different metal salts, however, the values of parameters were not reported consistent even for the same salt, e.g. the reported value of Ar was in the range of 10^{-3} to 10^{-2}, leading to up to one order of magnitude of difference on reaction rate. This is because that different authors applied different methods and systems to determine these kinetic parameters, and another possible reason is that the value of Ar can be temperature or pressure dependent so that more works should be conducted to get more sophisticated and accurate expression of Ar. The current study used the values of 0.003 and 1.0 of Ar and m for both adsorption and desorption processes as recommended by literature [22-24] for all working pairs in this study to have a fair comparison.

The heat convection equation of the flowing heat transfer fluid inside the tube is given as follows:

$$\rho_f c_{p,f} \frac{\partial T_f}{\partial t} + \rho_f c_{p,f} u \frac{\partial T_f}{\partial z} = \frac{1}{r}\frac{\partial}{\partial r}\left(r\lambda_f \frac{\partial T_f}{\partial r}\right) + \frac{\partial}{\partial z}\left(\lambda_f \frac{\partial T_f}{\partial z}\right) \quad (8)$$

where u is the flow velocity. The initial and boundary conditions are:

$$T|_{t=0} = T_{\mathrm{a}} \tag{9}$$

$$\left.\frac{\partial T_{\mathrm{f}}}{\partial r}\right|_{r=0,r_{\mathrm{s}}} = 0 \tag{10}$$

$$\left.\frac{\partial T}{\partial z}\right|_{z=0,L} = 0 \tag{11}$$

$$\lambda\left.\frac{\partial T}{\partial r}\right|_{r=r_{\mathrm{f}}} = h_{\mathrm{f}}\left(T_{\mathrm{f}} - T|_{r=r_{\mathrm{f}}}\right) \tag{12}$$

The heat transfer coefficients, h_{f} ($=\frac{Nu\lambda}{D}$), of forced tubular laminar and turbulent flows can be calculated by the following empirical equations [25]:

Laminar flow $$Nu = 4.36 \tag{13}$$

Turbulent flow $$Nu = 0.023Re^{0.8}Pr^{0.4} \tag{14}$$

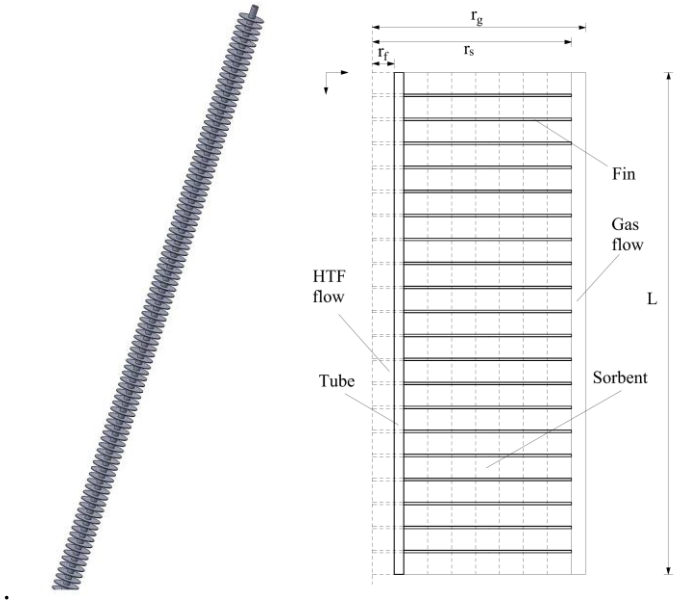

Figure 3 Physical model of ammonia chemisorption modular finned-tube heat exchanger.

2.5 Calculation method

The calculation framework is shown in Figure 4. For the charging process, the weather data between April and September was used to calculate the projected solar irradiance on the 20 m^2 tilted solar collector; the amount of solar heat effectively captured by the heat exchange fluid (water in this study)

can be calculated based on the solar collector thermal efficiency (Eqs. (1) and (2)); the amount of the stored heat in the forms of both sensible heat of the reactor and the solid adsorbent and the chemical potential energy of halide salt ammoniate-ammonia desorption can be calculated through the chemisorption simulation using Eqs. (4) - (13). Therefore, the maximum storage capacity of the solar heat by the chemisorption SSTES integrated with a 20 m^2 solar collector can be calculated, leading to the key parameter of the SSTES volume required and the storage capacity per unit area of the solar collector (kWh/m^2) for the integrated system.

In this work, the discharging process was simulated independently of the charging process. From the month October to March as the concentrated period of time with huge heating demand in the UK, the Eq. (3) was used to estimate the total space heating demand; with the given temperatures of the feed and return water for the targeted end-user heating facility, the required water flow rate can be calculated as the total heating demand is known; thereafter, the pre-defined return water temperature and the determined flow rate from heating facility can be used as the input parameters for the performance simulation of the SSTES: if the temperature of the hot water heated by the SSTES is lower than the required level, this hot water will be further heated by any available solar heat before finally being heated by a back-up boiler to the targeted level, the ratio of the delivered heat by the SSTES to the total heating demand is analyzed; otherwise, only operates the SSTES, the solar collector and the boiler would be in idle. Therefore, the maximum amount of heat release to be effectively used for the space heating can be calculated based on the real weather data of the ambient temperature, also leading to the corresponding volume value of the SSTES. Comparing the storage capacity estimated for the charging process and the discharging process, the solar collector area would need to be adjusted as well as the volume of the SSTES in order to match these two processes to construct a complete SSTES system. This will be discussed in the following section.

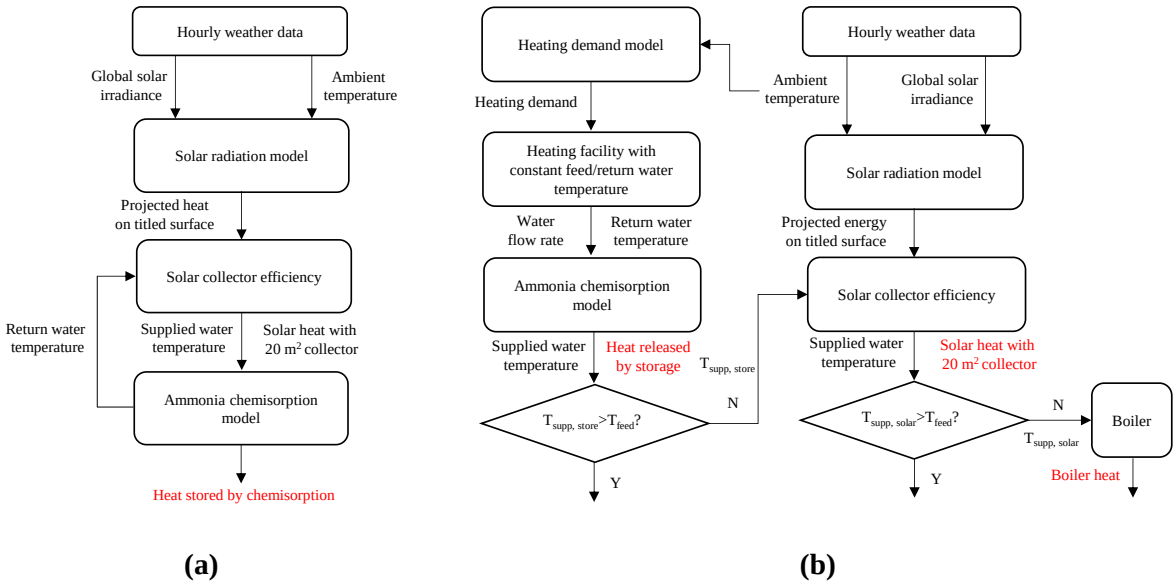

Figure 4 Calculation framework of current study, (a) charging process; (b) discharging process.

3 Results and discussions

3.1 Charing process

Figure 5(a) and (b) show the storage capacity of the SSTESs using different chemisorption working pairs, including $CaCl_2$-4/8NH_3, $BaCl_2$-0/8NH_3 and NaBr-0/5.25NH_3, coupled with a 20 m^2 solar collector, and the required storage system volume, as the function of the number of the modular reactor unit in charging group. Each chemisorption has a different threshold of desorption temperature to convert solar heat to chemical potential energy, and the varying efficiency of the studied two types of solar collectors over the effective desorption temperature range differentiate the performance of each chemisorption from the others. According to the thermodynamic equilibrium, the $CaCl_2$-4/8NH_3 chemisorption has the highest desorption temperature, followed by the $BaCl_2$-0/8NH_3 chemisorption, and the NaBr-0/5.25NH_3 chemisorption has the lowest, when under the same working pressure that is determined by the ammonia condensation in the condenser. On the other hand, the flat-plate collector has higher thermal efficiency in the low temperature range (e.g. <100 °C, based on 25°C ambient temperature and 1000 W/m^2 solar radiation) than the evacuated tube type, but it is opposite in the higher temperature range.

The increase of number of modular finned-tubes in one group allows more materials can be desorbed at the same time to harvest the solar heat as much as possible; however, because of the fixed solar

collector area and heat transfer fluid (water) flow rate, more finned-tubes in one group means lower water flow rate for each modular tube, therefore lower degree of conversion of desorption is achieved within one day, the reactor and adsorbent have to be re-heated the next day to achieve the required desorption temperature, hence relatively more solar heat is consumed as the sensible heat of the reactor and adsorbent. These opposite tendencies lead to an optimal number of modular finned-tubes in one group operation for each chemisorption case which gives the maximum storage capacity, as shown in Figure 5. The $CaCl_2$-4/8NH_3 chemisorption requires comparatively higher desorption temperature at which the flat-plate solar collector has lower efficiency than evacuated tube type. As a result, much less solar heat can be stored by the $CaCl_2$-4/8NH_3 chemisorption than that by the other two chemisorption regardless of the collector types; the maximum solar heat stored by the $CaCl_2$-4/8NH_3 chemisorption using evacuated tube collector almost double that of using flat-plate collector. For the other two chemisorption, the systems coupled with flat-plate solar collector performs slightly better than the ones using evacuated tube solar collector because the flat-plate type is more efficient in the domain of their desorption temperature.

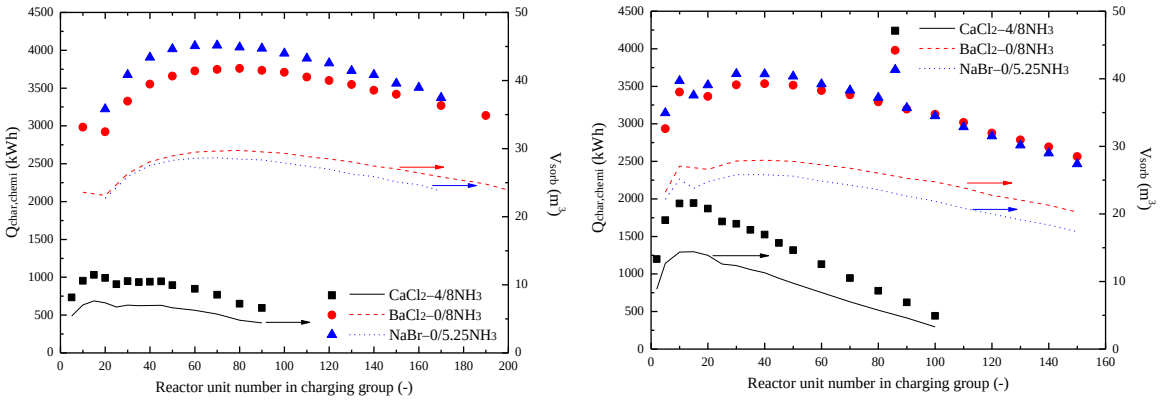

Figure 5 Stored solar heat by ammonia chemisorption and required storage volume, (a) using flat-plate solar collector; (b) using evacuated tube solar collector.

Table 3 summarizes the performance of the charging process with the maximum storage capacity, i.e. using the optimal numbers of the reactor unit. The stored chemical potential energy (sensible heat is not counted here), which is loss-free, are 1945kWh, 3746 kWh and 4066 kWh by using $CaCl_2$-4/8NH_3,

$BaCl_2$-0/8NH_3 and NaBr-0/5.25NH_3, respectively, which means the specific capacity per unit area of solar collector is 97.25 kWh/m^2, 187.3 kWh/m^2, and 203.3 kWh/m^2. The required storage volumes are 14.4 m^3, 29.6 m^3 and 28.6 m^3 respectively. It should be noted that the SSTES volume discussed here has taken into account of both the adsorbent material and any necessary system components involved, therefore, the obtained system energy densities are between 127-142 kWh/m^3, which are much lower than the pure salt material energy density in the range of 880-1485 kWh/m^3. This discrepancy is mainly attributed to three factors, the lower adsorbent bulk density comparing to pure salt density, the addition of expanded graphite as the porous supporting matrix, and the additional volume of other essential system components.

Despite of whether the discharging temperature is high enough or not for spacing heating, if these stored chemical potential energy can be 100% restored as the useful heat in the discharging process, to satisfy the total space heating demand of 9827 kWh from October to March, the required system volumes and the solar collectors should be accordingly adjusted to 72.76 m^3, 77.65 m^3 and 69.12 m^3, and 101m^2, 52.47m^2 and 48.34m^2, respectively.

Table 3 Performance of charging process using optimal group reactor number based on 20 m^2 solar collector.

Charging process	Modular reactor number in charging group	Stored energy (kWh)	Storage system volume (m^3)	Energy density (kWh/m^3)	Used solar collector
$CaCl_2$-4/8NH_3	15	1945	14.4	135	Evacuated tube
$BaCl_2$-0/8NH_3	70	3746	29.6	127	Flat-plate
NaBr-0/5.25NH_3	70	4066	28.6	142	Flat-plate

3.2 Discharging process

For the satisfactory delivery of the space heating, both the quantity and the quality of the discharged heat needs to meet the requirement. The storage capacity can be scaled up or down by proportionally

increasing/decreasing the number of solar collectors and enlarging/shrinking the storage system accordingly. However, the temperature threshold of the feed hot water is another issue. With the varying ambient temperature that sometimes could span a wide temperature range throughout the heating season, it is highly possible that when the ambient temperature is too low, even the fully charged SSTES cannot cover 100% heating demand by releasing adsorption heat to the return water and heating it to the desired temperature, i.e. the corresponding adsorption equilibrium temperature is insufficient to heat the return water up to the desired feed water temperature, or even worse that the adsorption temperature is lower than the return water temperature, as shown in Figure 6. This triggers the re-think of the selection of working salts, the equilibrium line of the preferable salt-ammonia reaction for SSTES application should be less sloping in the Clausius-Clapeyron *P-T* diagram, therefore the working salt can have relatively low desorption temperature resulting in high thermal efficiency of solar collector in summer, and sufficiently high adsorption temperature in winter to satisfy the requirement of space heating.

As shown in Figure 6, the adsorption temperatures of the chemisorption studied are fluctuating in the similar patent as the ambient temperature: the $CaCl_2$-4/8NH_3 adsorption temperature is always higher than the pre-fined return water of the radiator, therefore it has the potential of considerably contributing to the space heating; the NaBr-0/5.25NH_3 adsorption temperature curve is wiggling up and down the temperature line of the pre-defined low-temperature return water. In other words, the chemisorption SSTESs using unfavourable working pairs cannot solely operate to satisfy the heating demand no matter how much heat has been stored during the charging process, it only can partially contribute to the heating demand under relatively higher ambient temperature and still need supplementary heat such as from solar collector and back-up boiler in this study to lift up the temperature level of the feed water for proper heating. Therefore, the system size should be optimised by comparing the storage capacity in the charging stage and the delivery capacity in the discharging stage, avoiding large system design that contains much unreacted inoperative adsorbent. According to Figure 6, four different combinations of chemisorption and heating facilities are discussed here, including $CaCl_2$-4/8NH_3 and 70-40 °C radiator, $CaCl_2$-4/8NH_3 and 35-25 °C low temperature heating

facility, $BaCl_2$-0/8NH_3 and 35-25 °C low temperature heating facility, NaBr-0/5.25NH_3 and 35-25 °C low temperature heating facility.

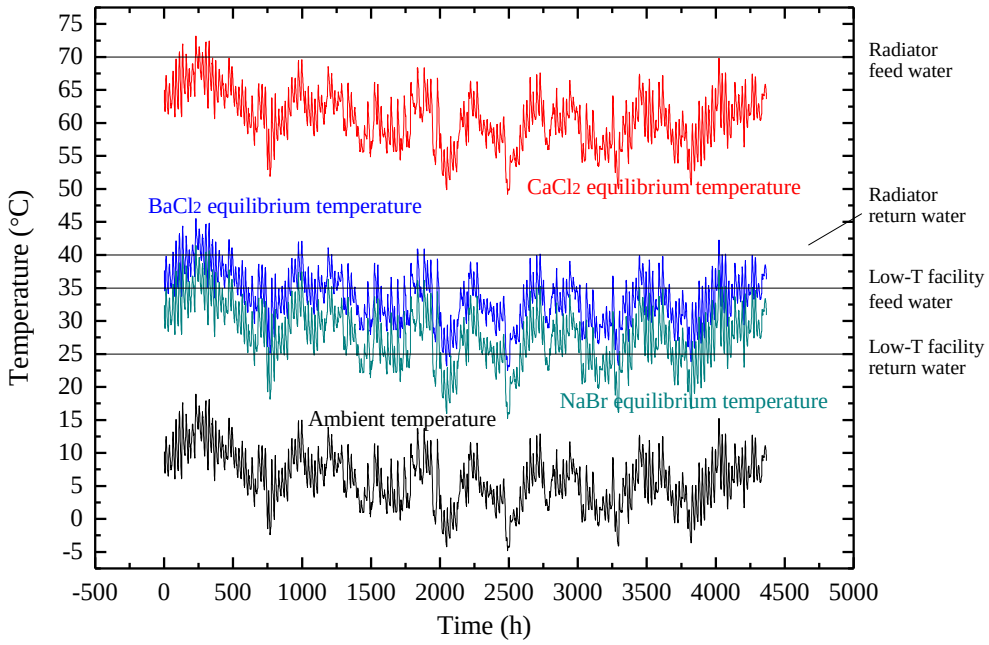

Figure 6 Ambient temperature and chemisorption equilibrium temperature with 1.0 bar equilibrium pressure drop in thermal discharging stage.

At the discharging stage, the adsorption heat from the SSTES, the solar heat from the solar collector and the boiler was utilized in consequence if necessary. It was found that solar heat utilised was quite few, less than 7% of the total heating demand in all study cases due to its nature of the limited availability during the months from October to March and being the back-up plan. The discharge performance is shown in Figure 7 as the function of the number of modular finned-tubes for one discharging group. As foregoing discussion, the hot water flow rate at the end-user heating facility is a fixed value when the heating demand and the feed and return hot water temperature are already given. Increasing the tube number in the discharging group results in an increase of the available adsorption heat at a time but a decrease of the water flow rate in each modular tube. With such inverse effect on two involved variables, there exists an optimal number of the modular tubes for one discharging group, and these optimal points for more compact system design are noticeable in Figure 7 and

summarized in Table 4. Using these optimal arrangement of discharging group, the volume of the storage system that can effectively deliver useful heat are compared to the volume needed to store 9827 kWh (100% heating demand) in charging stage is shown in Figure 8. The volume of a SSTES using hot water tank, based on the data of 54.4 kWh/m^3 storage density with 25% heat loss [3,6], to meet 100% space heating demand is presented as the bench mark for comparison. There shows the evident advantage of the chemisorption SSTESs with higher energy storage density than that of the hot water tank SSTES.

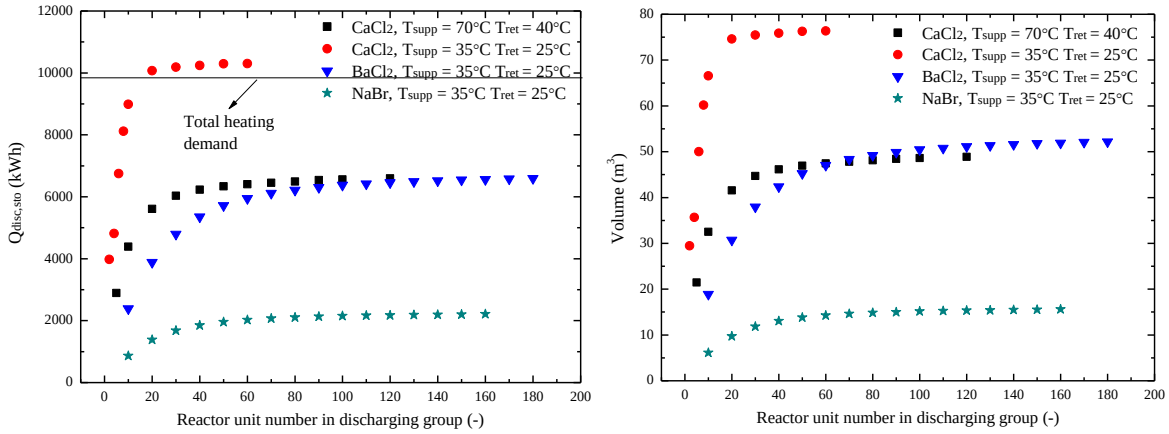

(a) **(b)**

Figure 7 Discharging performance of SSTES system, (a) heat released by ammonia chemisorption; (b) volume of storage system.

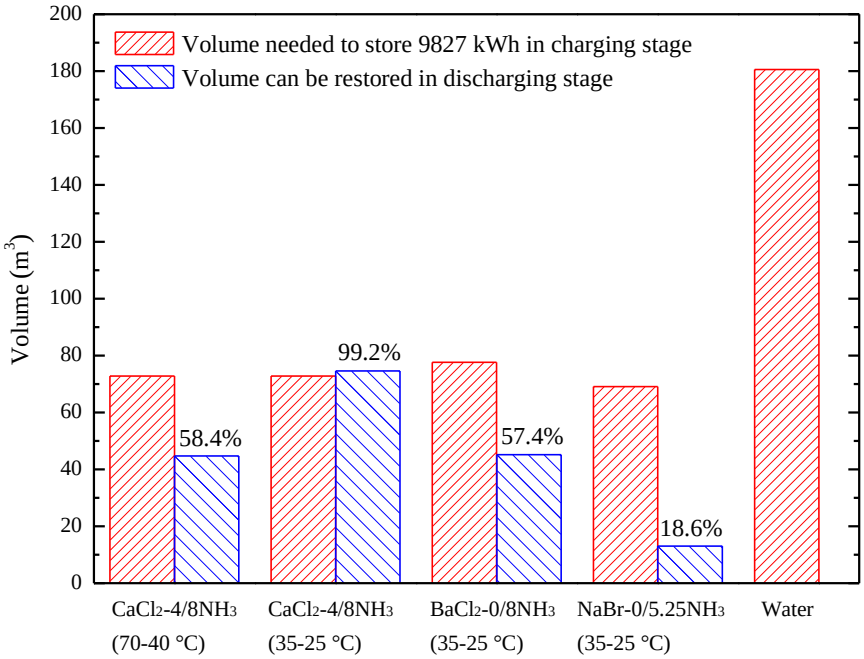

Figure 8 Comparison between SSTES volume needed to storage 9827 kWh in charging stage and volume can be restored in discharging stage, volume of water system was calculated based on 54.4 kWh/m^3 storage density considering 25% heat loss [3, 6].

As foregoing discussion, the $CaCl_2$-4/8NH_3 chemisorption has the higher equilibrium temperature among the studied cases when under the same working pressure. That means it can achieve higher adsorption temperature for the discharging, e.g. about 65 °C adsorption equilibrium temperature with ammonia evaporates at 5 °C. In this instance, the $CaCl_2$-4/8NH_3 SSTES can work well with either the conventional radiator (70-40 °C) or the low temperature heating facility (35-25 °C): the former combined heating system can deliver 59.4% of the total heating demand, while the latter one can achieve about 99.3%. As shown in Figure 7(a), for the case of the low temperature heating facility combined with the $CaCl_2$-4/8NH_3 SSTES, the total adsorption heat generated is higher than the total heating demand, nevertheless part of the adsorption heat is consumed as the sensible heat of the metallic reactor and solid adsorbent. Taking into account of the sensible heat consumption, to achieve 100% coverage of heating demand by a $CaCl_2$-4/8NH_3 SSTES, a minimum system volume of 74.6 m^3 and a minimum solar collector area of 103.6 m^2 is required, which seem unacceptable for one ordinary domestic dwelling.

The NaBr-0/5.25NH_3 chemisorption achieves the highest storage capacity in the charging stage since it has the lowest equilibrium temperature; because of the same reason, it performs the worst in the discharging stage as it has the lowest adsorption temperature, e.g. only about 25 °C equilibrium temperature with ammonia evaporated at 5 °C. Such adsorption performance fails to heat the return water for most of the time even for the low temperature heating facility. As a result, only 18.6% of the heating demand can be satisfied by the NaBr-0/5.25NH_3 SSTES.

Among all cases studied, the $BaCl_2$-0/8NH_3 chemisorption has moderate desorption/adsorption temperature therefore comparatively it reaches a balance between non-demanding desorption temperature at the charging stage and sufficient adsorption temperature at the discharging stage. If integrated with the low temperature heating facility, the $BaCl_2$-0/8NH_3 SSTES can contribute about 57.4% of the total heating demand with an additional 2.9% supplied by solar collector, and the rest of heating demand is met by a boiler. The required area of solar collector for such a coverage ratio is 30.5 m^2 which is a reasonable value for ordinary dwelling's roof installation. The required volume of the SSTES is 45.2 m^3, which seems still problematic, too large to be domestically applied. One straightforward solution is to reduce the system volume with smaller contribution of the SSTES and lower recovery of solar energy, which can still substantially reduce energy cost and carbon footprint of domestic households. The current study assumes the dwelling was maintained at 21 °C throughout the six months of the discharging stage, in fact, which is not necessary in reality; moreover, the heat loss of the dwelling can be significantly reduced by better insulation, then the SSTES system volume can be further reduced to an acceptable range. Radically, this issue can be alleviated through increasing the bulk density of the adsorbent (currently 450 kg/m^3), then further investigation is necessary to confirm the heat and mass transfer performance with high bulk density.

Table 4 Performance of discharging process using different heating facilities under optimal reactor unit umber in discharging group.

Discharging	Number of the modular tubes in	Chemisorption heat can be used [a]	Storage system	Coverage ratio by	Coverage ratio by	Required solar

	discharging group	(kWh)	volume (m^3)	SSTES (%)	solar (%)	collector area [b] (m^2)
$CaCl_2$-4/8NH_3 (70-40 °C)	30	6030	44.7	58.4	1.0	62.0
$CaCl_2$-4/8NH_3 (35-25 °C)	20	10072	74.6	99.2	0.1	103.6
$BaCl_2$-0/8NH_3 (35-25 °C)	50	5718	45.2	57.4	2.9	30.5
NaBr-0/5.25NH_3 (35-25 °C)	40	1847	13.0	18.6	7.0	9.1

[a] This heat was consumed as both sensible heat of adsorbent/reactor and useful heat of water heating.

[b] This area was calculated based on specific chemisorption charging capacity per unit area of solar collector obtained in charging stage.

4 Conclusions

The seasonal solar thermal energy storage using ammonia-based chemisorption for domestic application in the UK was studied in the current paper. Three different working pairs, $CaCl_2$-4/8NH_3, $BaCl_2$-0/8NH_3 and NaBr-0/5.25NH_3 were studied for chemisorption unit to be integrated with two different types of solar collector (flat-plate type and evacuated tube type) and two types of end-user heating facilities (high temperature radiator and low temperature floor heating/fan convector). The chemisorption modular reactors (finned-tube design) was heated or cooled group by group at both thermal charging and discharging stages. The selection of the chemisorption working pairs and the strategy of the group operation has been discussed for the optimal performance and system design. The major conclusions are:

(a) The preferable working pairs should have the less sloping equilibrium line in the Clausius-Clapeyron *P-T* diagram, meaning not only have relatively low desorption temperature that matches with the capability of the solar collectors, but also have sufficiently high adsorption temperature for space heating.

(b) The $CaCl_2$-4/8NH_3 chemisorption was capable to deliver 58.4% of the total heating demand when using conventional radiators, and deliver nearly 100% when using low-temperature heating facility, under the real weather condition during the months from October to March. To fully charge this amount of thermal energy at charging stage, the evacuated tube solar collector with the area of 62.0 m^2 and 103.6 m^2 and the SSTES with a volume of 44.7 m^3 and 77.6 m^3 were required, respectively, which could cause reluctance of employing such a SSTES for domestic application

(c) The NaBr-0/5.25NH_3 chemisorption can store most solar heat at thermal charging stage and had the largest energy density comparing to the other two working salts studied, however, the low adsorption temperature significantly limits its effectiveness at thermal discharge stage, only able to contribute about 18.6% of the heating demand when even using low-temperature heating facility.

(d) The $BaCl_2$-0/8NH_3 chemisorption had more preferable equilibrium temperature than the other two working pairs to reach the balance of non-demanding desorption temperature at thermal charging stage and moderate adsorption temperature at discharging stage. A $BaCl_2$-0/8NH_3 SSTES with a volume of 45.2 m^3 integrated with a 30.5 m^2 solar collector can cover 57.4% of the total heating demand when using low-temperature heating facility.

(e) The volume of the necessary system components has been taken into consideration in this work to discuss the storage energy density of the chemisorption storage systems, which was lower than the material-based value. Further investigation on the bulk density of the adsorbent composite with decent heat and mass transfer performance is worth more effort to significantly reduce the system volume.

Acknowledgement

The authors gratefully acknowledge the support from the Heat-STRESS project (EP/N02155X/1) and Centre for Energy Systems Integration (EP/P001173/1) funded by the Engineering and Physical Science Research Council.

Reference

[1] Department of Business, Energy & Industrial Strategy. Energy consumption in the UK 2017 Data Tables, London, UK, 2017.

[2] Jardine C, Lane K. Photovoltaics in the UK: An introductory guide for new consumers. Oxford: Environmental Change Institute 2003.

[3] Pinel P, Cruickshank CA, Beausoleil-Morrison I, Wills A. A review of available methods for seasonal storage of solar thermal energy in residential applications. Renewable and Sustainable Energy Review 2011; 15: 3341–3359.

[4] Mangold D, Schmidt T. The next generations of seasonal thermal energy storage in Germany. www.solites.de/download/literatur/07-Mangold_ESTEC%202007.pdf (Available May 2017).

[5] Fisch MN, Guigas M, Dalenback JO. A review of large-scale solar heating system in Europe. Solar Energy 1998; 63:355–366.

[6] N'Tsoukpoe KE, Liu H, Le Pierres N, Luo L. A review on long-term sorption energy storage. Renewable and Sustainable Energy Review 2009; 13: 2385–2396.

[7] Ma Z, Bao H, Roskilly AP. Feasibility study of seasonal solar thermal energy storage in domestic dwellings in the UK. Solar Energy 2018; 162:489–499.

[8] Li T, Wang R, Kiplagat JK, Kang Y. Performance analysis of an integrated energy storage and energy upgrade thermochemical solid-gas sorption system for seasonal storage of solar thermal energy. Energy 2013; 50:454–467.

[9] Li TX, Wu S, Yan T, Wang RZ, Zhu J. Experimental investigation on a dual-mode thermochemical sorption energy storage system. Energy 2017; 140:383–394.

[10] Jiang L, Wang R, Wang LW, Roskilly AP. Investigation on an innovative resorption system for seasonal thermal energy storage. Energy Conversion and Management 2017; 149:129–139.

[11] Bao HS, Oliveira RG, Wang RZ, Wang LW. Choice of low temperature salt for resorption refrigerator. Industrial & Engineering Chemistry Research 2010; 49:4897–4903.

[12] Skagestad B, Mildenstein P. District heating and cooling connection handbook. The International Energy Agency 1999.

[13] Myhren JA. Potential of ventilation radiators: performance assessment by numerical, analytical and experimental investigations. Doctoral Thesis, KTH, Sweden.

[14] Energy Saving Trust. Solar energy calculator sizing guide 2015. http://www.pvfitcalculator.energysavingtrust.org.uk/Documents/150224_SolarEnergy_Calculator_Sizing_Guide_v1.pdf (Access on 20/06/2018)

[15] Solar Rating and Certification Corporation. Directory of SRCC certified solar collector ratings. USA, 2007.

[16] Johnston D, Wingfield J, Miles-Shenton D. Measuring the fabric performance of UK dwellings. In: Proceedings of 26th Annual ARCOM Conference, 6–8 September 2010, Leeds, UK.

[17] Johnston D, Siddall M. The building fabric thermal performance of passivhaus dwellings-does it do what it says on the tin? Sustainability 2016; 8:97.

[18] An GL, Wang LW, Gao J, Wang RZ. A review on the solid sorption mechanism and kinetic models of metal halide-ammonia working pair. Renewable and Sustainable Energy Review 2018; 91:783–792.

[19] Wang RZ, Wang LW, Wu JY. Adsorption refrigeration technology: theory and application. John Wiley & Sons Singapore, 2014.

[20] Oliveira RG, Wang RZ, Kiplagat JK, Chen CJ. Novel composite sorbent for resorption systems and for chemisorption air conditioners driven by low generation temperature 2009; 34:2757–2764.

[21] Perry RH. Perry's chemical engineers' handbook, seventh edition. McGraw-Hill, New York, US.

[22] Dutour S, Mazet N, Joly JL, Platel V. Modeling of heat and mass transfer coupling with gas-solid reaction in a sorption heat pump cooled by a two-phase closed thermosyphon. Chemical Engineering Science 2005; 60:4093–4104.

[23] Azoumah Y, Neveu P, Mazet N. Optimal design of thermochemical reactors based on constructal approach. AIChE Journal 2007; 53:1257–1266.

[24] Le Pierrès N, Mazet N, Stitou D. Modelling and performances of a deep-freezing process using low-grade solar heat. Energy 2007; 32:154–164.

[25] Lienhard IV JH, Lienhard V JH. A heat transfer textbook, third edition. Phlogiston Press, 2006, USA.